International Journal Of Astrobiology
January 2017, Volume 16 Issue 1 Pages 82-90
http://dx.doi.org/10.1017/S1473550415000555
http://archimer.ifremer.fr/doc/00366/47678/

Irradiation effects on antibody performance in the frame of biochip-based instruments development for space exploration

Baque M. [1, *], Dobrijevic M. [2, 3], Le Postollec A. [2, 3], Moreau T. [4], Faye C. [5], Vigier F., Incerti S. [6, 7], Coussot G. [8], Caron J. [9], Vandenabeele Trambouze Odile [10, 11, 12]

[1] Univ Roma Tor Vergata, Dept Biol, Rome, Italy.
[2] Univ Bordeaux, LAB, UMR 5804, F-33270 Florac, France.
[3] CNRS, LAB, UMR 5804, F-33270 Florac, France.
[4] Univ Clermont Ferrand, INSERM U1103, GReD, CNRS UMR6293, Aubiere, France.
[5] Cap Alpha, COLCOM, F-34830 Clapiers, France.
[6] Univ Bordeaux, CENBG, UMR 5797, F-33170 Gradignan, France.
[7] CNRS, IN2P3, CENBG, UMR 5797, F-33170 Gradignan, France.
[8] Univ Montpellier, Inst Biomol Max Mousseron, Fac Pharm, CNRS,Unite Mixte Rech 5247, F-34093 Montpellier 5, France.
[9] Inst Bergonie, Dept Radiotherapy, Ctr Comprehens Canc, F-33076 Bordeaux, France.
[10] Univ Bretagne Occidentale, LMEE, UEB, IUEM UMR 6197, Plouzane, France.
[11] CNRS, IUEM UMR 6197, LMEE, Plouzane, France.
[12] IFREMER, UMR6197, LMEE, Plouzane, France.

* Corresponding author : M. Baqué, email address : mickael.baque@gmail.com

Abstract :

Several instruments based on immunoassay techniques have been proposed for life-detection experiments in the framework of planetary exploration but few experiments have been conducted so far to test the resistance of antibodies against cosmic ray particles. We present several irradiation experiments carried out on both grafted and free antibodies for different types of incident particles (protons, neutrons, electrons and C-12) at different energies (between 9 MeV and 50 MeV) and different fluences. No loss of antibodies activity was detected for the whole set of experiments except when considering protons with energy between 20 and 30 MeV (on free and grafted antibodies) and fluences much greater than expected for a typical planetary mission to Mars for instance. Our results on grafted antibodies suggest that biochip-based instruments must be carefully designed according to the expected radiation environment for a given mission. In particular, a surface density of antibodies much larger than the expected proton fluence would prevent significant loss of antibodies activity and thus assuring a successful detection.

Keywords : astrobiology, biochip, cosmic rays, search for extraterrestrial life

1. Introduction

Among the next tools to search for signs of past or present life in our Solar System, several instruments based on the biochip technology have been proposed in the framework of planetary exploration. A biochip is a miniaturized device composed of molecular recognition tools (or affinity receptors) like antibodies (Baqué *et al.* 2011b; de Diego-Castilla *et al.* 2011; Parro *et al.* 2005, 2011a; Sims *et al.* 2005, 2012) or aptamers (Baqué *et al.* 2011a), which allows the detection of hundreds of different compounds in a single assay. Widely developed for biotechnology use and medical or environmental diagnostics (see for example Wang 2006), miniaturized instruments based on biochips have been indeed proposed and studied for biosignature detection in an astrobiological context since more than 15 years (McKay *et al.* 2000; Parro *et al.* 2005; Le Postollec *et al.* 2007; Sims *et al.* 2005).

Mars, one of the most probable planetary body where to find signs of extinct or extant life outside of Earth, is the target of many upcoming dedicated missions: ESA-Roscosmos' ExoMars rover in 2016-2018, NASA's Mars2020 rover (a follow-up of to the Curiosity rover) and the Icebreaker mission concept proposed for a 2021 launch to be part of NASA's Discovery program (McKay *et al.*, 2013). Different space instruments based on the biochip technology and using antibodies have been proposed for these future missions: the Life Marker Chip (LMC) (Martins 2011; Sephton *et al.* 2013; Sims *et al.* 2012), and the Signs Of LIfe Detector (SOLID) (Parro *et al.* 2005, 2008, 2011a, 2011b). Another project, the Biochip for Organic Matter Analysis in Space (BiOMAS), proposes to combine both antibodies and aptamers in a single instrument (Baqué *et al.* 2011b, 2011a; Le Postollec *et al.* 2007). Recently, first in the framework of Mars2020 announcement of opportunity, and then in the framework of NASA's Discovery 2014 announcement of opportunity, these different teams have

united to work on the SOLID instrument proposal for the Icebreaker mission and thus to contribute with their different expertise to improve the technological readiness level of a biochip-based instrument for space exploration (Manchado *et al.* 2015; McKay *et al.* 2013; Smith & Parro 2014).

Indeed, although biochips are known to be very sensitive tools to detect specific target molecules, their sensitivity is related to the presence of functional affinity receptors. In order to develop a "space biochip", it is thus necessary to ensure that these biological receptors will survive space hazards. In particular, due to the very sparse data on this topic, it is important to determine the behavior of these biological receptors under cosmic particles irradiation.

Le Postollec *et al.* (2009a) performed simulations with the Geant4 Monte Carlo toolkit in order to estimate the radiation environment that a biochip would face if it were placed into a rover dedicated to explore Mars' surface. Ionizing doses accumulated and fluxes of particles entering the biochip have been established for both the Earth-Mars transit and the journey on Mars' surface. Neutrons and gammas appear as dominant radiation species on Mars' soil whereas protons dominate during the interplanetary travel. These results have been confirmed by other studies done by McKenna-Lawlor *et al.* (2012) and Derveni *et al.* (2012). Moreover, these simulations can today be confronted to the real radiation environment of an actual mission to Mars as it was monitored by the Radiation Assessment Detector (RAD) instrument on-board the Mars science laboratory spacecraft on cruise to Mars and continue to be recorded by the rover Curiosity directly on its surface (Hassler *et al.* 2013; Kim *et al.* 2014; Zeitlin *et al.* 2013). Indeed, the total cosmic radiation dose rate of 210 ± 40 μGy/day (Hassler *et al.* 2013) recorded at Gale Crater by Curiosity and the one measured inside the Mars Science Laboratory spacecraft during its cruise to Mars (481 ± 80 μGy/day) (Zeitlin *et al.* 2013) proved to

be in the same order of magnitude as model predictions with respectively ~840 µGy/day (without any shielding) for the Martian surface and ~240 µGy/day for the Earth-Mars transit considering only GCR (galactic cosmic rays) contribution (Le Postollec *et al.* 2009a).

Considering the lack of experimental data about cosmic rays effect on antibodies, particularly under lyophilized (freeze-dried) state, our team decided to investigate the effects of different types of particles at several energies. Our objective is first to study and measure cosmic rays effects on biological receptors and second to define well-adapted protections for a biochip-based instrument if we find evidences that cosmic rays might have deleterious effect on their performances. In a first study, Le Postollec *et al.* (2009b) performed neutrons irradiation on both antibodies and fluorescein dyes (used for detection of recognition events) at two energies (0.6 and 6 MeV) and with different fluences. Sample analyses demonstrated that, in tested conditions, neutrons do not affect antibody recognition capability and fluorescence dye intensity. More recently, the effects of 2 MeV protons on antibody performances (Baqué *et al.* 2011b) were investigated. These studies showed that this irradiation process did not affect the performances of antibodies as molecular recognition tools. In addition, printed antibody and Alexa-647 fluorescent dye were demonstrated to be stable between 1.18 and 1.33 MeV gamma radiation (de Diego-Castilla *et al.* 2011). Finally, Derveni *et al.* (2012) tested five antibodies freeze-dried in a variety of protective molecular matrices and exposed to 50 MeV protons. They showed that at a representative Mars-mission-dose, none of the antibodies studied exhibited any evidence of activity loss due to the radiation.

In the present paper, we broaden these previous studies to test the effect of electrons, carbon ions, protons (at different energies) and neutrons (at higher energies) on the recognition capability of antibodies (summarized in Fig 1). As protons and neutrons dominate the radiation environment during the Earth-Mars transit and on the Martian surface, we tested different high-energy particles from 15 to 50 MeV at different fluences. Moreover, other damaging particles are significantly present in cosmic and solar radiations such as carbon ions and electrons.

Chemicals and biological materials used to perform the experiments are given in section 2. Section 3 describes samples preparation, particles irradiation parameters and analysis protocols. Results are presented in section 4. The last section draws conclusions on this study.

2. Material

Monoclonal anti-Horseradish Peroxydase antibodies were obtained from Antibodies-online (Germany), Horseradish peroxydase (type II), O-Phenylenediamine dihydrochloride (OPD), NaH_2PO_4, Tween® 20, sodium acetate, sucrose, sodium azide, NaOH, H_2O_2, BSA, (L)-Histidine and (D)-Arginine L-tyrosinamide, fluorescein and Tris(hydroxymethyl) aminomethane were purchased from Sigma Aldrich (Saint-Quentin, France). NaCl and $MgCl_2$ were obtained from Chimie-Plus laboratoires (Bruyères de Pouilly, France) and Panreac Quimica (Barcelona, Spain), respectively. Chemicals were analytical grade and were used as received. DNA-Bind™ plates were obtained from Corning (Netherlands) and Maxisorp™ plates were obtained from VWR (France). Optical density of the reaction products was measured on a Tecan Infinite M200 microplate reader (Lyon, France) at 492 nm.

3. Method

3.1. Sample preparation

Our Biochip models are small polymer containers, called micro-wells, where antibodies samples are placed for the experiments. DNA-Bind™ plates were used for covalent grafting (N-Oxysuccinimide functionalization allows random amine binding, Moreau *et al.* 2011) whereas Maxisorp™ ones were used as sample containers for free antibodies. The samples preparation was done following the same protocol as in Baqué *et al.* (2011a).

Briefly, antibodies were irradiated under two different states: grafted and free. All samples were freeze-dried using the freeze-drying buffer described in Baqué *et al.* (2011a,b) and then sealed in a FoodSaver™ bag in dry atmosphere (silica gel was added in the bag) and stored in the dark at 4°C before irradiation. All irradiation effects were estimated on freeze-dried samples.

3.2. Irradiation parameters

3.2.1. Conditioning of samples during irradiation

In order to prevent potential degradations due to environmental changes (contact with air, moisture, potential organic contaminants, etc.), all samples were irradiated under their protecting packaging.

Micro-wells were irradiated directly in their sealed bags. The effect of the sealed bag, considering its thickness and composition, was assessed using simulations performed with the Geant4 toolkit (Agostinelli *et al.* 2003; Allison *et al.* 2006). We determined that the influence of the bag during irradiations was negligible as very few particles were stopped by this additional plastic layer and very few secondary particles were created (data not shown).

175

176 **3.2.2. Methodology adopted to choose irradiation parameters**

177 Numerical simulations give a basis to select the types of particles, energies and fluences
178 that we have to consider for irradiation experiments. However, this choice mainly
179 depends on technical constraints and the availability of irradiation facilities. As an
180 example, it is generally not possible to conduct ground-based experiments with the very
181 low flux of particles and the long duration of irradiation (months or years) encountered
182 in interplanetary space. In addition, due to analysis constraints (limit of detection,
183 uncertainties), it is also necessary to choose adequate irradiation parameters to ensure
184 that potential effects of particles on our targets will be measurable.
185 In the present study, when possible, we have chosen to use fluences in the same order of
186 magnitude as the surface density of grafted antibodies. The objective of our experiments
187 was to study the interaction between different types of particles and the antibody
188 molecule. Indeed, we wanted to determine if some particles could have a “direct effect”
189 on the recognition molecule: when a particle interacts with the molecule, is there
190 degradation or is the molecule completely insensitive to particle interaction? This
191 approach can allow the identification of particles and energies more deleterious to
192 antibodies (if existing) and the results obtained could help for studying the
193 implementation of biochips on further exploration missions whatever the target object in
194 the Solar System. For instance, it could give precious data on the shielding design that
195 must be developed considering the expected irradiation environment.

196

197 To determine the density of antibodies grafted into a well, we used an innovative
198 quantification technique called ADECA (Coussot *et al.* 2011a; Coussot *et al.* 2011b;
199 Moreau *et al.* 2011) that was well adapted to our purpose. The grafting density of

antibodies was defined around 8.8 x 10^{11} antibodies/cm^2 with roughly 2.8 x 10^{11} antibodies on the bottom and 5 x 10^{11} antibodies on the sidewalls.

The fluence of particles reaching the antibodies was assessed using numerical simulations performed with the Geant4 toolkit. Indeed, considering the geometry of the well, it is obvious that antibodies grafted on the sides do not receive the same fluence of particles as antibodies located at the bottom of the well. With a fluence of 3 x 10^{12} particles/cm², the fluence of particles on the sidewalls was derived from the Geant4 simulations to be 2.4 x 10^{-2} times the total fluence so 7.2 x 10^{10} particles/cm². Therefore, we can assess that 41% of antibodies grafted in a well have a significant chance to interact with at least one particle. With this method, direct effects of particles on antibodies can be detected if existing.

Lower fluences and higher fluences were also tested in some cases, with for example a fluence of protons ten times lower (3 x 10^{11} particles/cm^2) or a fluence of neutrons ten times higher (3 x 10^{13} particles/cm^2). In these cases, we estimate that 13% and 74% of grafted antibodies interacted with a particle respectively.

Free antibody samples were prepared at a concentration of 15 x 10^{16} antibodies/well. The exact disposition of antibodies into the well is not defined but it is assumed that they form several layers at the bottom of the well during freeze-drying. Therefore it is not possible to determine the number of antibodies that could interact with incident particles since each particle can penetrate in a column of piled antibodies.

3.2.3. Neutron irradiation

Neutron irradiation was performed at the cyclotron of Louvain-la-Neuve, in Belgium. The high flux neutron irradiation facility uses a primary 50 MeV deuteron beam on a

beryllium target. The energy spectrum of the outcoming neutron beam is dominated by a peak in the region of 23 MeV. The mean energy of neutrons is 16.56 MeV.

The current was set to 7 µA. Samples were positioned at two different distances so that they received two different fluences. At a 12 cm distance, the fluence was $F_H = 3 \times 10^{13}$ neutrons/cm² and the diameter of the beam was about 4.2 cm for 80% of homogeneity. Whereas at a 40.5 cm distance, the fluence was $F_L = 3 \times 10^{12}$ neutrons/cm² and the diameter of the beam was about 10.2 cm for 80% of homogeneity. Samples were irradiated during approximately 22 minutes.

3.2.4. Proton irradiation

Proton irradiation was also performed at the cyclotron of Louvain-La-Neuve, on the Light Ion Facility (LIF) (Fig. 2 Top). This mono-energetic proton beam line can produce up to 10^9 protons/cm²/s with energies from 10 to 75 MeV (Berger *et al.* 1997). The beam diameter is set to 10 cm and a ± 10% of homogeneity is ensured.

Three irradiation campaigns took place between June 2010 and June 2012. Our samples were irradiated with five different energies: 14.4 MeV, 20.9 MeV, 25.9 MeV, 29.4 MeV and 50.5 MeV. The proton flux was set to 5×10^8 protons/cm²/s so that the irradiations lasted 1h40min to reach the fluence of 3×10^{12} protons/cm² for all the tested energies and 10min to reach 3×10^{11} protons/cm² for 25.9 MeV and 50.5 MeV.

3.2.5. Electron irradiation

Electron irradiation was performed at the Institut Bergonié (Bordeaux, France) (Fig. 2 Bottom Left). The beam was calibrated to deliver 9 MeV electrons and it was scanned through a square collimator of 6 cm side. Samples were positioned at 1 m from the source. The flux delivered by the facility was 200 MU (Monitor Unit) per minute with 1 MU corresponding to 5.38×10^6 electrons impacting the bottom of the well (Gobet *et al.*

Submitted; unpublished data). Therefore, to deal with reasonable irradiation durations, we decided to irradiate samples during 70 minutes corresponding to a fluence of 2.35 x 10^{11} electrons/cm².

3.2.6. Carbon ions irradiation

Carbon ions irradiation was performed at the LNS (Laboratori Nazionali del Sud) facility of the INFN (Instituto Nazionale di Fisica Nucleare) in Catania. Samples were presented vertically in front of the beam. A specific mask was designed to fix the ELISA plate containing samples on a mobile device (Fig. 2 Bottom right) so that the whole plate could be irradiated at once without any intervention in the irradiation room.

The beam was scanned through a square collimator of 17 mm side. Calibration for the delivered dose has been done by means of a parallel plate ionization chamber. Radiochromic films have been also used for minimizing gaps and overlaps between irradiated areas in order to ensure a homogeneous irradiation of all samples.

The beam delivered ^{12}C ions with an energy of 62 MeV/nuc. For this experiment, the fluence applied was different from other experiments as it was not reasonable to reach 3 x 10^{12} carbon ions per cm² in an adequate delay and safe conditions. Therefore, we decided to study if energetic carbon ions could have an indirect effect on antibodies, i.e. if those particles of such energy could interact with the sample environment so that it could destabilize the whole system and degrade antibodies recognition performances. The fluence was set to 2.16 x 10^6 particles/cm² and was determined using results obtained with CREME 96 by Le Postollec *et al.* (2009a): it corresponds to the flux of ^{12}C 62 MeV/nuc ions at 1 A.U. (Astronomical Unit) delivered during 18 months (representing an upper limit for a Mars mission). The irradiation of each square area

lasted less than 20 seconds to reach the requested fluence so that the whole plate was irradiated within about 15 minutes.

3.3. Analysis protocol

3.3.1. Antibodies

After irradiation, analyses were performed in order to define the irradiation effects on the antibody performance. Protocols used here were detailed in previous studies (Baqué *et al.* 2011a) and are summarized below.

Grafted antibodies were analyzed with a direct ELISA test (Baqué *et al.* 2011a). This method, called A2HRP, focuses only on the recognition capability of the antibody's antigen binding site (epitope) and does not give an insight on the degradation of the entire antibody structure (Moreau *et al.* 2011). Briefly, the number of active antigen binding sites was measured by quantifying the amount of antigen (HRP) specifically retained by the antibodies. Indeed, the amount of HRP could be easily quantified using external standards of free HRP as we have demonstrated that the enzymatic reactivity of HRP was identical for free HRP, or HRP complexed to both free or grafted antibody (Moreau *et al.* 2011).

Free antibodies were analyzed with a competitive ELISA test (Baqué *et al.* 2011a). Briefly, in micro-well plates with freshly grafted anti-HRP antibodies, a defined amount of HRP is placed in competition with diluted amounts of irradiated samples or controls. After washing, the amount of HRP measured in the micro-well is inversely proportional to the amount of active antibody in the sample. Based on competitive curves, we calculated the half maximal inhibitory concentration (IC50). In our experiment, this

297 concentration represents the amount of competitive antibody that should be added to
298 inhibit 50% of antigen binding to grafted antibodies. Between two competitive
299 experiments, both HRP and grafted antibody concentrations are maintained identical.
300 Thus IC50 values are influenced by the affinity of competitive antibodies for the HRP.
301 If the apparent affinity of competitive antibodies is reduced, then the IC50 measured
302 will increase.

303 **3.3.2. Reference samples**

304 To evaluate the possible irradiation effects on our samples, different references and
305 controls were prepared. Irradiation effect on antibody was evaluated by comparing
306 irradiated samples to non-irradiated controls (NIC). NIC were treated simultaneously
307 and in the same manner as the irradiated samples, though they were not submitted to
308 irradiation. In order to estimate the effects of transport, temperature cycles and light
309 exposure on biochip performances, reference samples were used. These reference
310 samples (R4°C) were prepared at the same time as irradiated samples and NIC and were
311 stored in the laboratory at 4°C in the dark until analysis. As described by Baqué *et al.*
312 (2011a), all of the antibodies were freeze-dried using a specific buffer, which maintains
313 the anti-HRP antibody recognition capabilities after freeze-drying and during storage to
314 liquid reference levels. Results for grafted antibodies are therefore presented as
315 percentages of active antibodies for more clarity and in order to normalize all acquired
316 data during the several irradiation campaigns. This percentage is calculated by taking
317 the amount of HRP retained by NIC to 100%. NIC and R4°C were confronted for each
318 campaign to reflect any damage caused by transport, handling etc.

319 **3.3.3. Statistical treatment**

Irradiation effects were evaluated by comparing the mean signal values obtained for non-irradiated controls (NIC) and for irradiated samples. Thus, Student's t-tests were used to compare irradiated samples distribution and references distribution, taking into account the number of repetitions (from 4 to 18) and the standard deviation (SD) of each distribution. The differences between these two distributions were considered statistically significant with a 95 % level of confidence when the calculated *p*-values were below the 0.05 threshold value.

4. Results

4.1. Grafted antibodies

All the experiments performed on grafted antibodies are summarized in Table 1. This table presents the type, energy and fluence of particles tested. It also specifies the antibody grafting surface density allowing an assessment of the percentage of antibodies receiving at least one particle for each tested fluence. The percentage of antibodies still active after irradiation, calculated against non-irradiated controls (NIC), reveals possible degradation induced only by radiation exposure. Indeed, the effects of transport conditions are evaluated by confronting NIC with reference samples stored in the laboratory (R4°C), as described in paragraph 3.2.2. However, as for all the tested conditions NIC proved to be significantly equal to R4°C (not shown), only irradiation effects are presented here.

Irradiation on the other hand had different effects on the tested antibodies. Indeed, although no effect was detected with neutrons, electrons and ^{12}C, significant effects were observed with protons. Surprisingly, for high fluences, protons between 20 and 30 MeV significantly altered the antibody recognition performances, with losses around 30-35% and *p*-values between 10^{-4} and 10^{-8}, but not at lower and higher energies. Similarly, even at a lower fluence 25 MeV protons produced a significant recognition

loss, though limited to only 10-20%, whereas at 50 MeV no significant recognition loss was recorded. In our model the antibody surface density was maintained identical for the different exposure experiments therefore only 13% of antibodies should have received at least one particle at the lowest proton fluence against 42% at the highest. The protons' energy appears thus as a more damaging factor than the fluence, as only a certain energy range (20-30 MeV) produced significant damage to antibodies regardless of the fluence applied. However, by diminishing the ratio between the antibody surface density and the particles' fluence by a factor 3 (42% against 13% of antibodies receiving at least one particle between high and low fluences respectively) the effect of irradiation was greatly attenuated for 25 MeV protons (65% against 84% of active antibodies respectively).

The other tested particles did not induce significant changes in antibody recognition capabilities even at very high neutron fluence (3 x 10^{13} particles/cm²) or with heavy carbon ions at high energy (62MeV/n).

4.2. Free antibodies

Free antibodies were irradiated by 25 MeV and 50 MeV protons and 17 MeV neutrons at different fluences (3 x 10^{11} and 3 x 10^{12} particles/cm² for protons and 3 x 10^{12} and 3 x 10^{13} particles/cm² for neutrons). Results are summarized in Table 2. The irradiation effect was estimated following the methodology described in Baqué *et al.* (2011a). Briefly, when the half maximal inhibitory concentration (IC50) significantly increases, it indicates that in average, the antibodies have lost recognition capabilities since HRP has only one epitope to which the antibody binds (Moreau *et al.* 2011).

No modification of free antibody recognition capabilities under proton irradiations at 50 MeV was observed. However, at 25 MeV, we highlight here a significant recognition capability loss for free antibodies, leading to a significant increase in IC50 compared to the NIC. The increase in IC50 value indicates that, in average, the antibody activity has been deteriorated by 25 MeV protons irradiation leading to partial or complete antigen recognition site degradation. Based on a simplistic model, which considers that IC50 changes are only linked to a total loss of recognition capability, we can however estimate the percentage of active antibodies compared to non-irradiated controls as reported in Table 2. A maximum of 50% of antibodies appear to have lost their recognition capability when irradiated with a high fluence of 25 MeV protons. Although the other recorded changes in IC50 values after proton or neutron irradiation appear also quite high, with 20 to 30 % damaged antibodies (most notably after a high neutron flux), they were not significantly different from the controls. These results however point out a high variability in the samples, which can be problematic for repeatability measurements of future space instruments.

5. Discussion/Conclusion

Based on Monte Carlo simulations of the radiation environment faced by a biochip dedicated to explore Mars' surface (Le Postollec *et al.* 2009a), our team performed several ground-based irradiation experiments on biochip recognition molecules. Even though protons and neutrons clearly dominate the radiation spectrum during the Earth-Mars transit and on the Martian surface, other particles might be equally deleterious to biological molecules such as the antibodies used in biochips. Furthermore, a wide range of particle energy and fluence can be considered according to the envisaged mission to

Mars but also to other planetary bodies of interest in the Solar System. In the present study, the irradiation effects of protons, neutrons, electrons and carbon ions on the recognition capabilities of antibodies were therefore investigated at different energies and fluences. Two antibodies formulations were submitted to irradiation in order to broadly represent any future biochip-based space instruments as both grafted and free antibodies are considered. Our experimental approach consisted of using particle fluences in the same order of magnitude as grafted antibodies surface density in order to measure any damaging effect occurring when a particle interacts with an antibody.

Among the tested particles, only protons significantly altered the antibodies recognition capabilities. These damaging effects were however recorded only for a certain energy range between 20 and 30 MeV at both high and low fluences but confirmed for both formulations (free and grafted antibodies). Indeed, at higher and lower protons energies the antibodies recognition capabilities were not significantly altered. Irradiations of free antibodies lead moreover to a high variability in the estimated recognition capabilities of our antibodies samples.

Therefore, although the energy range of deleterious particles appears quite limited, a biochip instrument performance would not be affected for a typical mission to Mars, as the fluences of particles in this energy range will be significantly lower than the antibody surface density. However, this result underlines that attention must be paid to the ratio between antibody surface density and particles fluences expected for a given mission. The biochip instrument must be designed so that antibody surface density is much greater than incident protons fluence. Instrument shielding and/or antibodies grafting density should be consequently adapted.

In a similar ground-based study performed on five antibodies freeze-dried in different protective molecular matrices, Derveni *et al.* (2012) pointed out the more damaging role of processing and packaging than irradiation. Using doses of protons and neutrons at high energies (50 and 47 MeV respectively), comparable to the ones used in the present work, they did not detect any evidence of activity loss due to irradiation for a typical mission dose (10^{11} to 10^{12} protons/cm^2 and 10^7 to 10^8 neutrons/cm²). However, using 10^{13} protons/cm^2, most of the antibodies lost their activity. Thanks to these results they suggested that further shielding or alternative radiation protection approaches would need to be considered for long duration missions to other astrobiological targets. Our present work confirms this suggestion. We propose that the ratio between the fluence of protons and the surface density of antibodies has to be much lower than unity to prevent important loss of activity.

The main limitation of ground-based studies is that each constraint is generally studied individually and for a limited period of time that is not representative of a real space mission. In particular, the effect of cosmic rays is generally studied at a given energy (or a limited range of energies) and for one type of particle in a single experiment.

Moreover, additional constraints and hazards are expected for a space instrument. Long term storage, temperature variations, contamination risks, launch, landing and transportations vibrations and shocks should all be taken into account in the design and testing of a space dedicated instrument. For these reasons, a real space exposure of biochip prototypes has been attempted in the past by the LMC team for a short-term mission aboard the BIOPAN platform on a Russian Foton spacecraft (Derveni *et al.* 2013) and ground-based and field studies have been performed for the SOLID prototype (Parro *et al.* 2008; Sobrado *et al.* 2014). Furthermore, in the frame of the BiOMAS

444 project, biochip samples are currently exposed to real space conditions inside the
445 EXPOSE-R2 platform of ESA, part of the Photochemistry on the Space Station (PSS)
446 project, which was installed on the outside of the Zvezda module of the International
447 Space Station (ISS) in August 2014 (Vigier *et al.* 2013).
448 The long-duration exposure of the EXPOSE missions (Rabbow *et al.* 2009, 2012, 2015)
449 range from 12 to 18 months in the LEO environment of the ISS. The radiation
450 environment at this altitude, although not equivalent to interplanetary space or the
451 Martian surface, will allow anyway for a much better estimate of the long-term
452 resistance of immunoassays instruments for space applications.
453 Nevertheless, due to the high number of potentially hazardous factors encountered
454 during a space mission, ground-based studies are essential to isolate the most damaging
455 ones and thus propose adequate shielding or handling procedures.
456
457 Thus, our results from ground-based irradiation campaigns globally indicate that cosmic
458 rays might not alter the final performance of a biochip-based instrument in a typical
459 Martian mission, when antibodies are used as binders to detect the presence or the
460 absence of a target compound. The damaging effects of 20-30 MeV protons recorded in
461 the present study should not however be overlooked and further testing on-ground will
462 be necessary to support and interpret data from real space exposure missions.
463
464

465 ***Acknowledgments***

466 The research leading to these results has received funding from the European Union
467 Seventh Framework Programme FP7/2007-2013 under Grant Agreement no 262010 –
468 ENSAR.

We would like to thank the French National Space Agency (CNES) (Convention number DCT/SI/IM/2009-17733) and the Interdisciplinary CNRS program "Environnements Planétaires et Origines de la Vie" for financial support.

We also thank the Louvain-la-Neuve cyclotron facility staff, the Institut Bergonié staff and the staff from the Laboratori Nazionali del Sud of the Instituto Nazionale di Fisica Nucleare for their help during irradiation experiments.

References

Agostinelli, S. *et al.* (2003) Geant4—a simulation toolkit. *Nucl. Instrum. Methods Phys. Res. Sect. Accel. Spectrometers Detect. Assoc. Equip.*. **506**(3), 250–303.

Allison, J. *et al.* (2006) Geant4 developments and applications. *IEEE Trans. Nucl. Sci.*. **53**(1), 270–278.

Baqué, M. *et al.* (2011a) Investigation of Low-Energy Proton Effects on Aptamer Performance for Astrobiological Applications. *Astrobiology*. **11**(3), 207–211.

Baqué, M., Le Postollec, A., Coussot, G., Moreau, T., Desvignes, I., Incerti, S., Moretto, P., Dobrijevic, M., & Vandenabeele-Trambouze, O. (2011b) Biochip for astrobiological applications: Investigation of low energy protons effects on antibody performances. *Planet. Space Sci.*. **59**(13), 1490 – 1497.

Berger, G., Ryckewaert, G., Harboe-Sorensen, R., & Adams, L. (1997) Cyclone–A multipurpose heavy ion, proton and neutron see test site. In *1997 RADECS Conference Data Workshop*. p. 51.

Coussot, G., Faye, C., Ibrahim, A., Ramonda, M., Dobrijevic, M., Postollec, A., Granier, F., & Vandenabeele-Trambouze, O. (2011) Aminated dendritic surfaces characterization: a rapid and versatile colorimetric assay for estimating the amine density and coating stability. *Anal. Bioanal. Chem.*. **399**(6), 2295–2302.

Coussot, G., Perrin, C., Moreau, T., Dobrijevic, M., Postollec, A.L., & Vandenabeele-Trambouze, O. (2011) A rapid and reversible colorimetric assay for the characterization of aminated solid surfaces. *Anal. Bioanal. Chem.*. **399**(3), 1061–1069.

Derveni, M., Allen, M., Sawakuchi, G.O., Yukihara, E.G., Richter, L., Sims, M.R., & Cullen, D.C. (2013) Survivability of Immunoassay Reagents Exposed to the Space Radiation Environment on board the ESA BIOPAN-6 Platform as a Prelude to Performing Immunoassays on Mars. *Astrobiology*, 130103060450009.

Derveni, M., Hands, A., Allen, M., Sims, M.R., & Cullen, D.C. (2012) Effects of Simulated Space Radiation on Immunoassay Components for Life-Detection Experiments in Planetary Exploration Missions. *Astrobiology*. **12**(8), 718–729.

de Diego-Castilla, G., Cruz-Gil, P., Mateo-Martí, E., Fernández-Calvo, P., Rivas, L.A., & Parro, V. (2011) Assessing Antibody Microarrays for Space Missions: Effect of Long-Term Storage, Gamma Radiation, and Temperature Shifts on Printed and Fluorescently Labeled Antibodies. *Astrobiology*. **11**(8), 759–773.

Gobet, F. *et al.* (Submitted) Experimental and Monte Carlo absolute characterization of a medical electron beam. *Radiat. Meas.*

514 Hassler, D.M. *et al.* (2013) Mars' Surface Radiation Environment Measured with the
515 Mars Science Laboratory's Curiosity Rover. *Science*, 1244797.

516 Kim, M.-H.Y. *et al.* (2014) Comparison of Martian Surface Radiation Predictions to
517 the Measurements of Mars Science Laboratory Radiation Assessment Detector
518 (MSL/RAD). In American Geophysical Union Fall 2014 Meeting. San
519 Francisco, CA, United States.

520 Manchado, J.M., Sebastián, E., Romeral, J., Sobrado-Vallecillo, J., Herrero, P.L.,
521 Compostizo, C., Gómez-Elvira, J., & Parro, V. (2015) SOLID SPU: A TRL 5-6
522 Sample Preparation Instrument for Wet Chemistry Analysis on Mars. In Lunar
523 and Planetary Science Conference. p. 1222.

524 Martins, Z. (2011) In situ biomarkers and the Life Marker Chip. *Astron. Geophys.*.
525 **52**(1), 1.34–1.35.

526 McKay, C.P. *et al.* (2013) The Icebreaker Life Mission to Mars: A Search for
527 Biomolecular Evidence for Life. *Astrobiology*. **13**(4), 334–353.

528 McKay, D.S., Steele, A., Allen, C., Thomas-Keptra, K., Schweitzer, M.H., Priscu, J.,
529 Sears, J., Avci, R., & Firman, K. (2000) Mars immunoassay life detection
530 instrument (MILDI). *Lunar Planet Inst Contrib*. (1062 Part 2), 219–220.

531 McKenna-Lawlor, S., Gonçalves, P., Keating, A., Reitz, G., & Matthiä, D. (2012)
532 Overview of energetic particle hazards during prospective manned missions to
533 Mars. *Planet. Space Sci.*. **63–64**(0), 123–132.

534 Moreau, T., Faye, C., Baqué, M., Desvignes, I., Coussot, G., Pascal, R., &
535 Vandenabeele-Trambouze, O. (2011) Antibody-based surfaces: Rapid
536 characterization using two complementary colorimetric assays. *Anal. Chim.*
537 *Acta*. **706**(2), 354–360.

538 Parro, V. *et al.* (2005) Instrument development to search for biomarkers on mars:
539 Terrestrial acidophile, iron-powered chemolithoautotrophic communities as
540 model systems. *Planet. Space Sci.*. **53**(7), 729–737.

541 Parro, V. *et al.* (2008) SOLID2: an antibody array-based Life-detector instrument in a
542 Mars drilling simulation experiment (MARTE). *Astrobiology*. **8**(5), 987–999.

543 Parro, V. *et al.* (2011a) Classification of Modern and Old Rio Tinto Sedimentary
544 Deposits Through the Biomolecular Record Using a Life Marker Biochip:
545 Implications for Detecting Life on Mars. *Astrobiology*. **11**(1), 29–44.

546 Parro, V. *et al.* (2011b) SOLID3: a multiplex antibody microarray-based optical sensor
547 instrument for in situ Life detection in planetary exploration. *Astrobiology*.
548 **11**(1), 15–28.

549 Le Postollec, A. *et al.* (2007) Development of a Biochip dedicated to planetary
550 exploration. First step: resistance studies to space conditions. In *Journées SF2A*
551 *2007 Semaine de l'Astrophysique Française 2007*.

Le Postollec, A. *et al.* (2009a) Monte Carlo Simulation of the Radiation Environment Encountered by a Biochip During a Space Mission to Mars. *Astrobiology*. **9**(3), 311–323.

Le Postollec, A., Coussot, G., Baqué, M., Incerti, S., Desvignes, I., Moretto, P., Dobrijevic, M., & Vandenabeele-Trambouze, O. (2009b) Investigation of Neutron Radiation Effects on Polyclonal Antibodies (IgG) and Fluorescein Dye for Astrobiological Applications. *Astrobiology*. **9**(7), 637–645.

Rabbow, E. *et al.* (2009) EXPOSE, an astrobiological exposure facility on the International Space Station - from proposal to flight. *Orig. Life Evol. Biospheres*. **39**(6), 581–598.

Rabbow, E. *et al.* (2012) EXPOSE-E: an ESA astrobiology mission 1.5 years in space. *Astrobiology*. **12**(5), 374–386.

Rabbow, E. *et al.* (2015) The astrobiological mission EXPOSE-R on board of the International Space Station. *Int. J. Astrobiol.*.**14**(1), 3–16.

Sephton, M.A., Sims, M.R., Court, R.W., Luong, D., & Cullen, D.C. (2013) Searching for biomolecules on Mars: Considerations for operation of a life marker chip instrument. *Planet. Space Sci.*. **86**, 66–74.

Sims, M., Cullen, D., Bannister, N., Grant, W., Henry, O., Jones, R., McKnight, D., Thompson, D.P., & Wilson, P. (2005) The specific molecular identification of life experiment (SMILE). *Planet. Space Sci.*. **53**(8), 781–791.

Sims, M.R. *et al.* (2012) Development status of the life marker chip instrument for ExoMars. *Planet. Space Sci.*. **72**(1), 129–137.

Smith, H. & Parro, V. (2014) Planetary Protection Plan for an Antibody based instrument proposed for Mars2020. In 40th COSPAR Scientific Assembly. p. 3140.

Sobrado, J.M., Martín-Soler, J., & Martín-Gago, J.A. (2014) Mimicking Mars: A vacuum simulation chamber for testing environmental instrumentation for Mars exploration. *Rev. Sci. Instrum.*. **85**(3), 035111.

Vigier, F. *et al.* (2013) Preparation of the Biochip experiment on the EXPOSE-R2 mission outside the International Space Station. *Adv. Space Res.*. **52**(12), 2168–2179.

Wang, J. (2006) Electrochemical biosensors: Towards point-of-care cancer diagnostics. *Biosens. Bioelectron.*. **21**(10), 1887–1892.

Zeitlin, C. *et al.* (2013) Measurements of Energetic Particle Radiation in Transit to Mars on the Mars Science Laboratory. *Science*. **340**(6136), 1080–1084.

589 **Figure legends**

590 **Fig. 1:** Simulated spectra of particle fluxes, as a function of energy, during the Earth-
591 Mars transit (left) and at Mars' surface (right) with the energy range of particles
592 investigated in this study (red zone). This figure is an adaptation of Fig. 8 in Le
593 Postollec *et al.* (2009a).

594 **Fig. 2: Top:** Proton irradiation using the Light Ion Facility (LIF) at the cyclotron of
595 Louvain-la-Neuve. The source is located on the left in this picture and the samples are
596 placed on the right behind a metal slide with a 10 cm diameter hole. Several removable
597 disks are placed between the source and the samples to allow the modulation of protons
598 energy. **Bottom Left:** Picture of the facility at the Institut Bergonié where samples were
599 irradiated with 9 MeV electrons. **Bottom Right:** Mobile device developed to ensure the
600 ELISA plate motion during carbon ions irradiation at LNS (Catania).

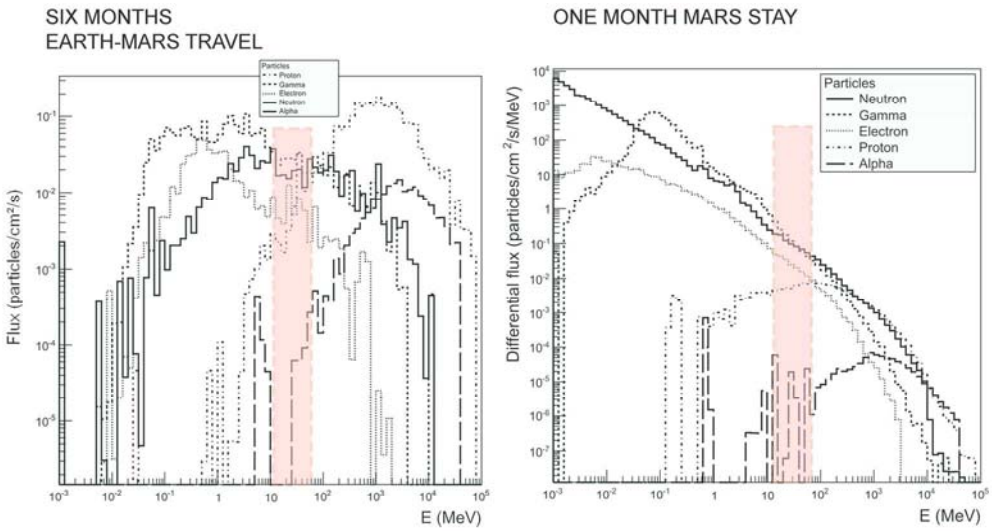

Tested particles and energies

Proton: 15, 20, 25, 30, 50 MeV
Neutron: 17 MeV
Electron: 9 MeV
Carbon: 62 MeV/n

143x98mm (300 x 300 DPI)

99x124mm (300 x 300 DPI)

Table 1. Influence of neutron, proton, electron and carbon radiation effects on grafted antibodies recognition capability at different fluences. The percentages of active antibodies were normalized using the NIC that were thus fixed at 100%. The percentage of antibodies receiving at least one particle was calculated according to the antibody surface density, the tested fluence and the sample geometry. SD, standard deviation; *n* is the number of measurements. *p*-value < 0.05 (in bold) indicate samples that are different to NIC at 95 % of confidence.

	Protons							Neutrons		Electrons	^{12}C
Fluence particles/cm²	3×10^{11}		3×10^{12}						3×10^{13}	2.3×10^{11}	2.2×10^{6}
Energy MeV	25	50	15	20	25	30	50	17 (mean energy)		9	62 MeV/n
Antibodies receiving at least 1 particle % *	13		41						88	10	< 1
Percentage of active antibodies % ± SD (*n*)	84 ± 9 (13)	89 ± 10 (5)	97 ± 19 (15)	62 ± 7 (5)	65 ± 12 (13)	73 ± 8 (5)	92 ± 14 (5)	100 ± 7 (4)	96 ± 4 (5)	98 ± 4 (4)	102 ± 10 (10)
p-value	**6.98×10^{-4}**	0.083	0.612	**4.7×10^{-4}**	**3.95×10^{-8}**	**6.47×10^{-4}**	0.283	0.938	0.136	0.656	0.839

* Antibody surface density is equal to 8.8×10^{11} Ab/cm² for all experiments.

Table 2. Influence of neutron and proton irradiation on free-antibody recognition capability at different fluences. IC50 (µg/mL), half maximal inhibitory concentration; SD, standard deviation; *n* is the number of measurements. The percentages of active antibodies were estimated in comparison with NIC. *p*-values < 0.05 (in bold) indicate samples that are different to non-irradiated controls at 95 % of confidence.

	Protons				Neutrons		Non-irradiated controls (NIC)
Fluence particles/cm²	3 x 10^{11}		3 x 10^{12}		3 x 10^{13}		
Energy MeV	25	50	25	50	17 (mean energy)		
IC 50 (µg/mL) ± SD (n)	3.1 ± 0.2 (4)	4.1 ± 1.0 (7)	4.7 ± 1.0 (7)	3.8 ± 0.8 (8)	3.2 ± 0.2 (4)	4.2 ±1.4 (8)	3.2 ± 0.6 (18)
Percentage of active antibodies %	100	71	50	79	105	73	100
p-value	0.946	0.059	**0.004**	0.085	0.666	0.163	